Chemistry–A European Journal
Research Article
doi.org/10.1002/chem.202301218
Chemistry Europe
European Chemical Societies Publishing
www.chemeurj.org

From Framework to Layers Driven by Pressure – The Monophyllo-Oxonitridophosphate β-$MgSrP_3N_5O_2$ and Comparison to its α-Polymorph

Reinhard M. Pritzl,[a] Nina Prinz,[a] Philipp Strobel,[b] Peter J. Schmidt,[b] Dirk Johrendt,[a] and Wolfgang Schnick*[a]

Abstract: Oxonitridophosphates exhibit the potential for broad structural diversity, making them promising host-compounds in phosphor-converted light-emitting diode applications. The novel monophyllo-oxonitridophosphate β-$MgSrP_3N_5O_2$ was obtained by using the high-pressure multi-anvil technique. The crystal structure was solved and refined based on single-crystal X-ray diffraction data and confirmed by powder X-ray diffraction. β-$MgSrP_3N_5O_2$ crystallizes in the orthorhombic space group *Cmme* (no. 67, $a = 8.8109(6)$, $b = 12.8096(6)$, $c = 4.9065(3)$ Å, $Z = 4$) and has a structure related to that of $Ba_2CuSi_2O_7$. DFT calculations were performed to investigate the phase transition from α- to β-$MgSrP_3N_5O_2$ and to confirm the latter as the corresponding high-pressure polymorph. Furthermore, the luminescence properties of Eu^{2+} doped samples of both polymorphs were investigated and discussed, showing blue and cyan emission, respectively (α-$MgSrP_3N_5O_2$; $\lambda_{max} = 438$ nm, *fwhm* = 46 nm/2396 cm^{-1}; β-$MgSrP_3N_5O_2$; $\lambda_{max} = 502$ nm, *fwhm* = 42 nm/1670 cm^{-1}).

Introduction

Oxonitridophosphates such as AE_2PO_3N (AE = Ca, Sr, Ba) or $Sr_3P_6O_6N_8$ were recently discussed as potential host compounds in phosphor-converted light-emitting diode applications.[1–3] Such mixed-anion compounds often crystallize in various structure types owing to increased flexibility of formal charges through substitution of N^{3-} by O^{2-}. This is useful for tuning the luminescence properties, since a fundamental change in emission usually requires a change in the host lattice or, more importantly, of the activator environment. In contrast to that the doping concentration affects emission only slightly.[4,5] Thus, there is great incentive to explore oxonitridophosphates, since the isoelectronic relationship of P/N to Si/O is expected to result in a similar structural diversity and therefore a variety for host structures as known for silicates. This structural similarity is evident from the oxonitride parent compound PON, which exhibits a number of SiO_2 analogous high-pressure/high-temperature (HP/HT) modifications.[6,7] Theoretically, there are several strategies to generate new host lattices in the compound class of oxonitridophosphates. One possibility of fundamentally changing the host structure is to modify the degree of condensation κ (i.e. the atomic ratio of the central atoms (P) : ligands (N/O)). Another one is to change the ligand ratio at an existing κ, since oxygen is usually twofold cross-linked and nitrogen can be triply- or even fourfold-connected in nitridic compounds.[8] Hence, O/N substitution theoretically allows for a by far higher number of charge balanced compositions with different cation ratio CR = counter cation : network cation, at a constant κ. This affects significantly the physical properties, such as stability due to a more covalent character of P–N-bonds.[9] Within the context of luminescent materials engineering, increased electron density in between activator ion and ligand leads to a stronger nephelauxetic effect.[10] However, only a few oxonitridophosphates have been investigated so far. Primarily, this is due to the challenging synthesis originating from the low thermal stability of phosphorus nitrides (e.g. P_3N_5) and the difficulty of controlled oxygen incorporation.[11–13] The so-called "azide approach" has proven to be successful for the synthesis of numerous nitridophosphates under high-pressure. Adding PON as an oxygen source has also shown this route to be suitable for oxonitridophosphate synthesis.[14] The thermolysis of the azide leads to an increase of the N_2 partial pressure in the reaction crucible and, according to Le Chatelier, to a suppression of the decomposition of the phosphorus (oxo)nitrides.[3,15] Another successful approach is the combination of "nitride and mineralizer-route". This strategy has been revived and modified recently by Eisenburger *et al.* for synthesis of transition metal oxonitridophosphates, starting from binary nitride precursors like ScN and TiN by adding NH_4F as activation reagent.[16,17]

[a] R. M. Pritzl, N. Prinz, Prof. Dr. D. Johrendt, Prof. Dr. W. Schnick
Department of Chemistry
University of Munich (LMU)
Butenandtstraße 5–13, 81377 Munich (Germany)
E-mail: wolfgang.schnick@uni-muenchen.de
[b] Dr. P. Strobel, Dr. P. J. Schmidt
Lumileds Phosphor Center Aachen (LPCA)
Lumileds (Germany) GmbH
Philipsstraße 8, 52068 Aachen (Germany)

Supporting information for this article is available on the WWW under https://doi.org/10.1002/chem.202301218

Based on this, a combination of both nitride and azide approaches, appears to be a promising method to synthesize new oxonitridophosphates, as exemplified by the synthesis of $MgSrP_3N_5O_2$. The latter was obtained starting from stoichiometric amounts of Mg_3N_2, $Sr(N_3)_2$, PON and P_3N_5, as well as NH_4Cl as mineralizer, performed under HP/HT conditions (6 GPa, approx. 1270 K).[14] With a degree of condensation $\kappa = 3/7$, $MgSrP_3N_5O_2$ contains a condensed anionic 3D network structure. In contrast, a number of related isoelectronic nitrides, oxonitrides and oxides show layered structure types for $\kappa = 3/7$ (e.g. $RE_2P_3N_7$ (RE = La, Ce, Pr, Nd, Sm, Eu, Ho, Yb), $RE_2Si_3O_3N_4$ (RE = La, Nd, Sm, Gd, Dy, Ho, Er, Yb), $AE_3P_6O_6N_8$ (AE = Sr, Ba), $Ca_2MgSi_2O_7$ and $SrHoAl_3O_7$).[3,18–22] This observation was our starting point to search for a corresponding layered polymorph of $MgSrP_3N_5O_2$. In this contribution, we report on the synthesis and structure elucidation of the novel β-polymorph of $MgSrP_3N_5O_2$. DFT calculations were performed to investigate the phase transition from α- to β-$MgSrP_3N_5O_2$ and to confirm the latter as the corresponding high-pressure polymorph. In the context of phosphor research, the obtained products were characterized and the luminescence properties of Eu^{2+} doped samples were investigated, compared and related to each other.

Results and Discussion

Synthesis

As described in literature α-$MgSrP_3N_5O_2$ can be prepared by a HP/HT reaction at 6 GPa and approx. 1270 K using a hydraulic multianvil press starting from Mg_3N_2, $Sr(N_3)_2$, amorphous a-PON, and P_3N_5 according to Equation (1):[14]

$$Mg_3N_2 + 3\ Sr(N_3)_2 + 6\ \text{a-PON} + P_3N_5 \rightarrow 3\ \alpha\text{-}MgSrP_3N_5O_2 + 8\ N_2 \quad (1)$$

We found out, that replacing a-PON by P_4O_{10} enables the synthesis of crystallographically phase-pure α-$MgSrP_3N_5O_2$ at 3 GPa and temperatures up to 1670 K (Equation (2)), which was confirmed by Rietveld refinement of powder X-ray diffraction data (Figure S1, Table S1, Supporting Information).

$$5\ Mg_3N_2 + 15\ Sr(N_3)_2 + 3\ P_4O_{10} + 11\ P_3N_5 \rightarrow 15\ \alpha\text{-}MgSrP_3N_5O_2 + 40\ N_2 \quad (2)$$

P_4O_{10} is less condensed ($\kappa = 2/5$) therefore more reactive than PON ($\kappa = 1/2$). Moreover, under these synthesis conditions, it is present in liquid form and thus acts as a flux.[23]

Using cristobalite type cri-PON instead of a-PON and increasing the reaction pressure to 7 GPa, the HP modification β-$MgSrP_3N_5O_2$ can be prepared as main phase. However, the preparation of β-$MgSrP_3N_5O_2$ starting from P_4O_{10} at these reaction pressures was not possible. Highest yields can be achieved by using MgO and cri-PON as oxygen sources (according to Equation (3)).

$$3\ MgO + 3\ Sr(N_3)_2 + 3\ \text{cri-PON} + 2\ P_3N_5 \rightarrow 3\ \beta\text{-}MgSrP_3N_5O_2 + 8\ N_2 \quad (3)$$

The title compounds were isolated as air- and moisture-stable grayish solids. After washing with de-ionized water, crystals with edge lengths up to 20 μm were obtained (Figure S2).

Crystal structure of β-$MgSrP_3N_5O_2$

The crystal structure of β-$MgSrP_3N_5O_2$ was solved and refined based on single-crystal X-ray diffraction data in the orthorhombic space group *Cmme* (no. 67) with lattice parameters a = 8.8109(6), b = 12.80960(6) and c = 4.9065(3) Å. The crystallographic data are given in Table 1, Wyckoff positions, atomic coordinates, anisotropic displacement parameters, as well as interatomic distances and angles are given in Tables S3–S5.

Table 1. Crystallographic data from single-crystal refinement of β-$MgSrP_3N_5O_2$.

Formula	β-$MgSrP_3N_5O_2$
Crystal system	orthorhombic
Molecular weight/g mol^{-1}	306.89
Space group	*Cmme* (no. 67)
Lattice parameters/Å	a = 8.8109(6), b = 12.8096(6), c = 4.9065(3)
Cell volume/Å^3	553.77(6)
Formula units per cell	4
Calculated density/g cm^{-1}	3.681
μ/mm^{-1}	10.660
T_{min}/T_{max}	0.8908/1.0000
Radiation	Mo-K_α (λ = 0.71073 Å)
Temperature/K	293(2)
F(000)	584
θ range/°	$2.806 < \theta < 43.069$
Total no. of reflections	6716
Independent reflections ($>2\sigma$)	582 (526)
Refined parameters	37
R_{int}; R_σ	0.0552; 0.0206
$R1$ (all data); $R1$ ($F^2 > 2\sigma(F^2)$)	0.0317; 0.0270
$wR2$ (all data); $wR2$ ($F^2 > 2\sigma(F^2)$)	0.0597; 0.0582
Goodness of fit	1.061
$\Delta\rho_{max}$; $\Delta\rho_{min}$/e·Å^{-3}	0.664; −0.968

Additional solid-state ^{31}P MAS NMR spectroscopy experiments support the structure solution (Figure S3). In the spectrum two signals with an intensity ratio of 2:1 are observed, which can be assigned to the two crystallographic sites (P1: Wyckoff 8*m*; P2: Wyckoff 4*b*). The chemical shifts δ_1 = 10.4 and δ_2 = 5.4 ppm (Figure S4) are in a typical range for oxonitridophosphates.[24,25]

The nitrogen content was determined by CHNS elemental analysis (Tables S6). For SEM-EDX measurements (Table S2) only the atomic cation ratios were considered (Sr/Mg/P), since partial hydrolysis during water treatment falsifies both the anion and total atomic values. Both, measured cationic values as well as ratios agree well with the theoretical ones. Based on the

obtained structure model, a Rietveld refinement based on powder X-ray diffraction data was carried out to check the sample for phase purity and phase content (Figure 1, Table S7).

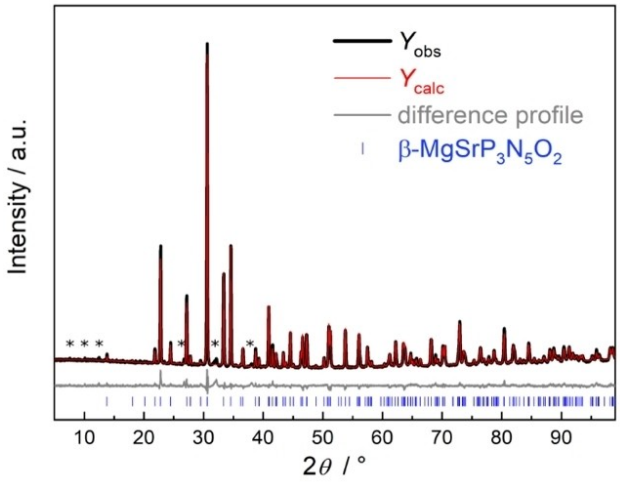

Figure 1. Rietveld refinement based on PXRD data of β-$MgSrP_3N_5O_2$ with experimental data (black line), calculated diffraction pattern (red line), corresponding difference profile (gray line) and related Bragg reflections (vertical blue bars). Reflections of an unknown byproduct are marked with asterisks.

Additional reflections of an unknown minor side phase are marked with asterisks in Figure 1.

In contrast to many textbook examples, a pressure-driven reduction in the dimensionality of the anionic partial structure is observed in the case described here.[26–28] α-$MgSrP_3N_5O_2$ forms a 3D framework structure, whereby β-$MgSrP_3N_5O_2$ prepared under higher pressure can be classified as a monophyllo-oxonitridophosphate following silicate nomenclature, which consists of monolayers of $P(O,N)_4$ tetrahedra and thus has a two-dimensional structure. According to the nomenclature introduced by Liebau, *vierer* and *sechser* rings of condensed $P(O,N)_4$ tetrahedra occur in both polymorphs (Figure 2). In the case of α-$MgSrP_3N_5O_2$ additional *achter* rings connect *vierer* and *sechser* rings, resulting in the 3D arrangement.[29]

Further information about the crystal structure of the α-type see Pucher *et al.*.[14] In β-$MgSrP_3N_5O_2$ the anionic $P(O,N)_4$ tetrahedra layer exhibits two different P sites. Respective Q^3-type PON_3 tetrahedra (O terminally bound) and all-side vertex sharing Q^4-type PN_4 tetrahedra (all N bridging) occur in an atomic ratio of 2:1. This stands in good agreement to Pauling's 2nd rule, where the N atoms prefer the bridging positions, while the O atoms are terminally bound to P.[31–33] The Rietveld refinement as well as lattice energy calculations (MAPLE), bond valence sums (BVS) and charge distribution (CHARDI) calculations (Tables S8 and S9) support the unambiguous assignment of O an N in the structure model.[34–38] The resulting topology of the anionic framework specified by the point symbol $\{4.6^2\}_2\{4^2.6^2.8^2\}$ (calculated with TOPOS), has been assigned once for nitridophosphate based compounds in bex-REP_3N_7 (topological symbol defined by *Reticular Chemistry Structure Resource* (RCSR)).[39,40]

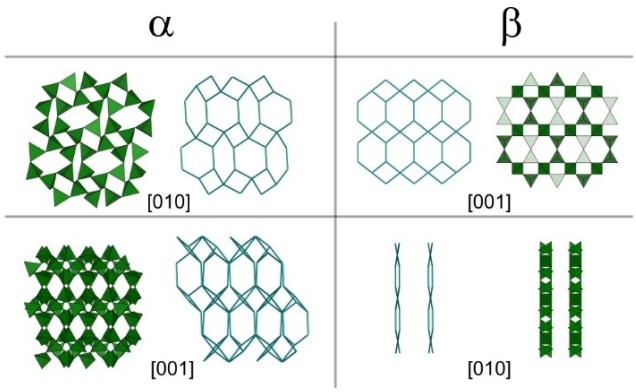

Figure 2. Comparison of the anionic $P(O,N)_4$ motifs of both $MgSrP_3N_5O_2$ polymorphs (left side α-type, right side β-type) with respective topological representation. Each connection line in the topological representation exemplifies a P–N–P bond. Top: *sechser* and *vierer* rings viewed along [010] (α-type) and [001] (β-type); bottom: framework structure (α-type) viewed along [001] versus layers (β-type) along [010].[30]

The monolayers in bex-REP_3N_7, which crystallizes in the $Ba_2CuSi_2O_7$ structure type, are shifted one-half of a *b*-translation against each other, whereas in β-$MgSrP_3N_5O_2$ the monolayers are stacked congruently (Figure 3).[18,41] Therefore, the layered

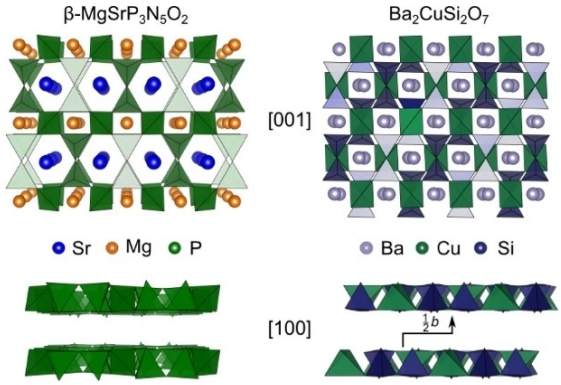

Figure 3. Comparison of the structures of β-$MgSrP_3N_5O_2$ (left side) and $Ba_2CuSi_2O_7$ (right side) along [001] as well as [100]. Here, both stacking and displacement along the *c* translation are visualized.[30]

structure expected for $\kappa = 3/7$ represents a hitherto unprecedented structure type. The anionic layers of β-$MgSrP_3N_5O_2$ are separated by Sr^{2+} and Mg^{2+} ions in the interstitial spaces of different ring-types created by the $P(N,O)_4$ tetrahedra connection pattern. Sr^{2+} ions prefer the larger *sechser* ring positions, and Mg^{2+} cations prefer the smaller *vierer* ring positions, due to their differing ionic radii (Figures 3 and 4).[29,42]

Thereby, Mg occupies a single crystallographic site located in a slightly compressed octahedron. This is due to the occupation of the axial octahedral corners by O and the equatorial ones by N. This is noticeable by the axial Mg–O bond lengths of 2.117(3) Å, which are slightly shorter than the

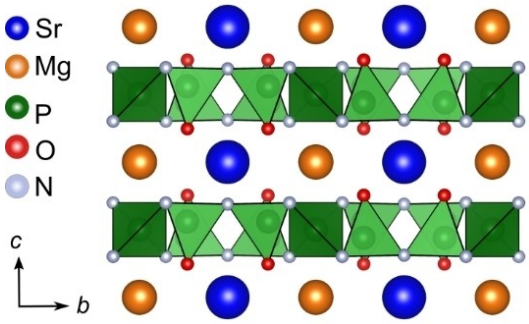

Figure 4. Mg (orange) and Sr (blue) cations separated through anionic oxonitridophosphate layers, view along [100].[30]

equatorial Mg–N bond lengths with 2.1845(19) Å (Figure 5). Sr is surrounded by four O and six N atoms, in a pentagonal

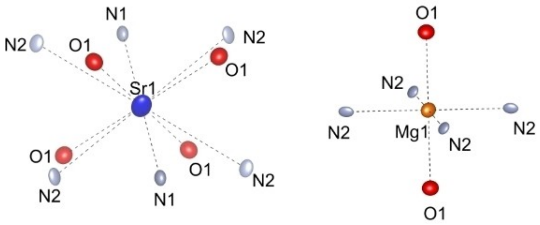

Figure 5. Coordination of Sr and Mg atoms in β-$MgSrP_3N_5O_2$. Sr atom is illustrated in blue, Mg atom in orange, O atoms in red, and N atoms in gray (displacement parameters with 95% probability.[30]

antiprismatic coordination. The Sr–N (2.680(3)–2.8402(19) Å) and Sr–O (2.9071(15) Å) distances are in the same range as reported for other strontium oxonitridophosphates (e.g. Sr_2PO_3N and $Sr_3P_6O_6N_8$) and correspond well with the sum of the ionic radii.[2,3,42]

Density functional theory calculations

The comparison of the α- and β-polymorphs shows several indications that β-$MgSrP_3N_5O_2$ is a high-pressure phase of α-$MgSrP_3N_5O_2$. The β-type is synthesized at higher pressures, exhibits a smaller cell volume (553.77(6) $Å^3$ versus 562.06(10) $Å^3$) while maintaining $Z=4$ (=higher density), and shows a higher coordination at the Sr site ($CN=10$ versus $CN=9$) which is consistent with Neuhaus' pressure-coordination rule.[43] To confirm the assumed high-pressure phase transition correlation from α- to β-$MgSrP_3N_5O_2$, additional ab initio DFT calculations were performed. The structure optimization was obtained through relaxation of atom positions and cell parameters. The energy-volume curves were computed by simulating a synthesis pressure up to 8 GPa. The enthalpy as a function of pressure is depicted in Figure 6, as extracted from the energy-volume curves evaluated with the Universal Equation of States.[44]

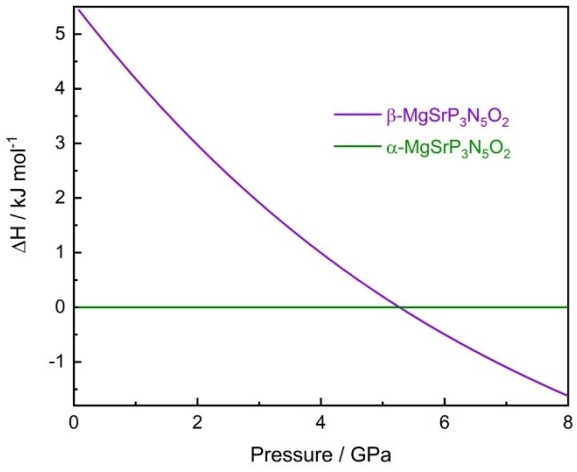

Figure 6. Enthalpy-pressure diagram obtained by fitting the Universal Equation of States from Energy-Volume diagram for the α- and β-polymorph.

The enthalpy difference as a function of pressure shows an energetic favouring of β-$MgSrP_3N_5O_2$ compared to the α-type for a pressure above 5.3 GPa. The intersection of both curves herein indicates a possible phase transition, which, however, has not been observed experimentally as yet.

UV/Vis reflectance spectroscopy

To characterize the optical properties an undoped sample of β-$MgSrP_3N_5O_2$ was investigated by diffuse reflectance spectroscopy (Figure S4). For determination of the optical band gap, the Kubelka–Munk function $F(R)=(1-R)^2/2R$, where R represents the reflectance, was used to convert the reflectance spectrum into a pseudo-absorption spectrum.[45] Via Tauc plot (plot of $h\nu$ versus $(F(R)\cdot h\nu)^{1/n}$), an approximately linear region is evident for $n=1/2$, which indicates a direct band gap (Figure 7).[46] By applying a tangent to the inflection point in this range and determination of the intersection with the abscissa, a band gap of about 5.1 eV was estimated.

Photoluminescence properties

To investigate luminescence properties of both modifications, samples were prepared by addition of $EuCl_2$ as dopant to the starting mixtures (approx. 3 mol% Eu^{2+} with respect to Sr^{2+}). Upon irradiation with UV light ($\lambda_{exc.}=420$ nm) α-$MgSr_{0.97}P_3N_5O_2{:}0.03Eu^{2+}$ shows blue emission with a maximum at 438 nm and a full width at half-maximum (*fwhm*) of 46 nm/2396 cm^{-1}. In contrast, β-$MgSr_{0.97}P_3N_5O_2{:}0.03Eu^{2+}$ shows a strong cyan emission with 502 nm and *fwhm*=42 nm/1620 cm^{-1} (Figure 9). The observed luminescence can be explained by comparing the cationic coordination spheres. In both cases, only one luminescence signal is evident, which is consistent with the presence of one crystallographic Sr site, and

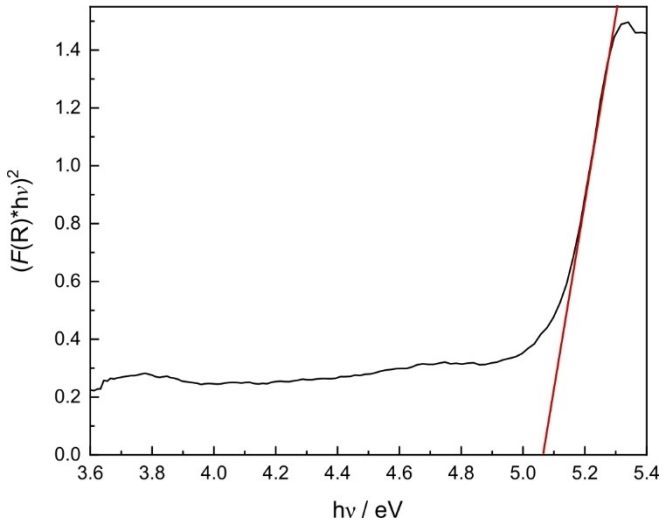

Figure 7. Tauc plot of non-doped β-$MgSrP_3N_5O_2$ (black line) with a tangent at the inflection point (red line).

the ionic radii indicate that Eu^{2+} occupies preferably only Sr^{2+} sites rather than Mg^{2+} sites.[3,47] In α-$MgSrP_3N_5O_2$, Sr is reported to be coordinated by a doubly capped pentagonal bipyramid (see Figure 8).[14]

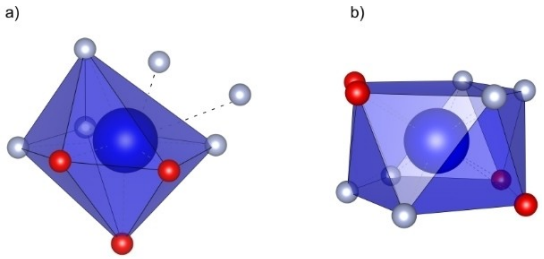

Figure 8. Coordination of the Sr site in α-$MgSrP_3N_5O_2$ (a) and β-$MgSrP_3N_5O_2$ (b). Sr atoms are illustrated in blue, O atoms in red and N atoms in gray.[30]

Therefore, the coordination number (*CN*) is 7 + 2 (3×O and 6×N). In contrast, in β-$MgSrP_3N_5O_2$ Sr exhibits a pentagonal antiprismatic coordination (*CN* = 10; 4×O and 6×N). Sr is in both polymorphs located at the Wyckoff position 4*e*. However, the site in β-$MgSrP_3N_5O_2$ exhibits a higher symmetry (2/*m* versus 1). This contributes to a narrowing of the emission band, caused by a reduction of the lattice relaxation around the activator ion in its excited state due to the higher site symmetry, which can be seen in the reduction of the full width at half maximum from 46 nm/2396 cm^{-1} (α-$MgSr_{0.97}P_3N_5O_2$:0.03Eu^{2+}) to 42 nm/1620 cm^{-1} (β-$MgSr_{0.97}P_3N_5O_2$:0.03Eu^{2+}).[48–50] This can be explained by symmetry-induced smaller bond length variance in β-$MgSrP_3N_5O_2$, which is $\sigma^2 = 0.0069$ (symmetry-related three different Sr–N/O distances; Table S5) versus $\sigma^2 = 0.048$ (nine different Sr–N/O distances) in α-$MgSrP_3N_5O_2$.[51] Furthermore, the observed red-shift ($\lambda_{max} = 438$ nm (α-type) to $\lambda_{max} = 502$ nm (β-type)) can be attributed to the nephelauxetic effect as well as ligand field splitting, whereby essentially the former was considered here (see Figure 9).

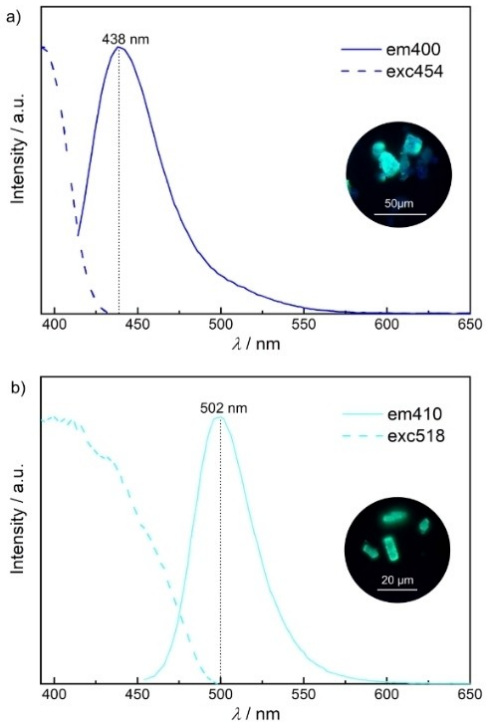

Figure 9. Excitation (dashed line) and emission spectra (continuous line) of α-$MgSr_{0.97}P_3N_5O_2$:0.03Eu^{2+} (a) and β-$MgSr_{0.97}P_3N_5O_2$:0.03Eu^{2+} (b), inset: micrograph of luminescent particles.

Consideration of the closest ligands of the first coordination sphere of the activator ion (< 2.85 Å Eu^{2+}–N/O distance) may serve as explanation: In the α-type, only three nitrogen atoms and two oxygen atoms are located in close proximity (see Figure 10 a), while in the β-type, six nitrogen atoms coordinate

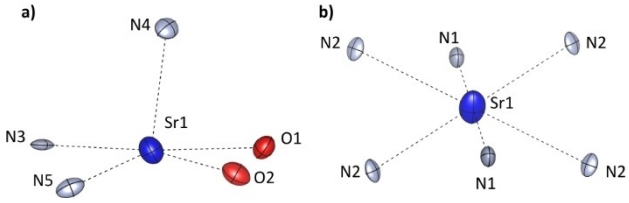

Figure 10. Next neighbour coordination of the activator site (O/N distances ≤ 2.85 Å to Sr) in both polymorphs. Sr atoms in blue, O atoms in red, N atoms in gray (displacement parameters with 95% probability). a) Sr site in α-$MgSrP_3N_5O_2$, b) Sr site in β-$MgSrP_3N_5O_2$.[30]

most closely (Figure 10 b). The smaller electronegativity of nitrogen compared to oxygen leads to an increased covalency of the Eu–N bond, which results in an energetic lowering of the

Eu^{2+} 5*d* levels and therefore a reduction of the 4*f*–5*d* transition energy.[52,53] The higher nitrogen content in the first coordination sphere of Eu^{2+} in β-$MgSr_{0.97}P_3N_5O_2$:$0.03Eu^{2+}$ should lead to an enhanced nephelauxetic effect and thus to a stronger reduction of the 4*f*–5*d* transition energy, which leads to the observed red-shift of both, lowest lying absorption and emission bands.

A classification of both compounds as (oxo)nitridophosphate based phosphors shows that α-$MgSr_{0.97}P_3N_5O_2$:$0.03Eu^{2+}$ exhibits emission comparable to $SrSiP_3N_7$:Eu^{2+} ($\lambda_{max} = 430$ nm, *fwhm* = 53 nm/2731 cm^{-1}), while β-$MgSr_{0.97}P_3N_5O_2$:$0.03Eu^{2+}$ represents the most narrow cyan emitting (oxo)nitridophophate based phosphor known so far, compared to other (oxo)nitridophosphate based phosphors such as Ca_2PO_3N:Eu^{2+} ($\lambda_{max} = 525$ nm, *fwhm* ≈ 4025 cm^{-1}).[2,54]

Conclusion

In this contribution, we have reported on synthesis and structural investigation of the high-pressure polymorph β-$MgSrP_3N_5O_2$ as well as a comparison to its low-pressure α-modification $MgSrP_3N_5O_2$ and the structurally similar silicate $Ba_2CuSi_2O_7$. DFT calculations revealed an energetic preference of the β-polymorph at elevated pressure, a possible transition from α- to β-$MgSrP_3N_5O_2$ at 5.3 GPa and confirm the latter as the corresponding high-pressure polymorph. In addition, an alternative synthesis protocol for α-$MgSrP_3N_5O_2$ was developed. Luminescence properties of Eu^{2+}-doped samples of both polymorphs were investigated. The different luminescence behaviour was compared and explained. For a more detailed consideration, MO calculations could be performed on both compounds in subsequent work.[55] In terms of a potential application, β-$MgSrP_3N_5O_2$ fills the so called cyan gap (480–520 nm) that commonly occurs in phosphor-converted white light-emitting diodes (pc-wLED).[56,57] Based on the luminescence properties of the literature known α-polymorph, the subject of subsequent work could be the fundamental investigation of known alkaline earth (oxo)nitridophosphates with respect to their luminescence behaviour when doped with Eu^{2+}. In summary, we were able to synthesize and structurally elucidate a novel oxonitridophosphate by comparing structural motifs of literature known compounds with $\kappa = 3/7$. A possible approach to explore further (oxo)nitridophosphates could be to focus on other compounds that share the same degree of condensation however exhibit completely different structural behaviour (e.g. 3D vs. layers, chains vs. isolated units).

Experimental Section

Synthesis of P_3N_5: In accordance to Stock and Grüneberg semi-crystalline phosphorus(V) nitride was prepared through ammonolysis of P_4S_{10} (approx. 7.0 g, Sigma-Aldrich 99.99%) with ammonia (Air Liquide, 5.0) at 850 °C in a fused silica boat, placed in a quartz tube.[58] To ensure anhydrous conditions, the apparatus (including the fused silica boat) was pre-heated for 5 h at 1000 °C under reduced pressure (10^{-3} mbar). Subsequently, the silica boat was loaded with P_4S_{10} in an argon counterflow. The apparatus was saturated with NH_3 for 4 h (constant flow of approx. 3.6 $L\,h^{-1}$), heated with a rate of 5 °C min^{-1} to 850 °C, held for 4 h and cooled to ambient temperature with a rate of 5 °C min^{-1}. After flushing the apparatus with Ar for 1 h (in order to remove remaining NH_3) the product was obtained as orange colored grains. P_3N_5 was identified by powder X-ray diffraction, FTIR spectroscopy and CHNS analysis.

Synthesis of cri-PON: Cristobalite type phosphorus oxonitride was synthesized by a modified solid-state reaction of stoichiometric amounts of P_3N_5 and P_4O_{10} according to Kingma *et al.* using a hot isostatic press (HIP, AIP6-30H, American Isostatic Presses, Inc., Columbus, Ohio, USA).[59] The synthesis was carried out under N_2 (99.9%) atmosphere at 100 MPa and 780 °C. For this purpose, the starting materials were ground in an agate mortar and filled into a W crucible, which was placed in an Al_2O_3 over-vessel. The assembly was transferred into the HIP and the apparatus was purged three times. Then a pressure booster (Maximator, DLE-5-30-2) was used to build up the necessary pre-pressure for operating the main-compressor. The pressure was increased to 50 MPa at 20 °C, followed by heating the sample up to 780 °C (heating-rate: 5 °C min^{-1}), resulting in a final pressure of 100 MPa. The reaction condition was maintained for 10 h and subsequently allowed to cool down to 20 °C (cooling-rate: 5 °C min^{-1}) before releasing the remaining pressure manually. The product was obtained as a grayish sinter cake, which was investigated for phase purity by powder X-ray diffraction and CHNS analysis.

Synthesis of $Sr(N_3)_2$: Strontium azide was synthesized by an ion exchange reaction of $SrCO_3$ (Sigma Aldrich, 99.995%) with aqueous HN_3 using a cation exchanger (Amberlyst 15) according Suhrmann *et al.*.[60,61] HN_3, formed by passing an aqueous solution of NaN_3 (Acros Organics, 99%, extra pure) through the cation exchanger, was carefully dropped into an aqueous suspension of the carbonate until the eluate exhibited pH neutrality. Residues of the carbonate respectively impurities of the starting materials were filtered off and the solvent was removed by rotation evaporation. The product was obtained as crystalline colorless needles, which were investigated for phase-purity by powder X-ray diffraction. **Caution**: HN_3 is explosive in dry form and highly poisonous, special care is mandatory.

Synthesis of α-/β-$MgSrP_3N_5O_2$: The oxonitridophosphate polymorphs α-/β-$MgSrP_3N_5O_2$ were synthesized via high-pressure high-temperature synthesis using a 1000 t press with a modified Walker-type multianvil apparatus.[62–64] Both products were synthesized from stoichiometric amounts of P_3N_5, $Sr(N_3)_2$, Mg_3N_2, cri-PON respectively P_4O_{10}. Doping of both compounds was carried out by partial substitution of Sr^{2+} with Eu^{2+} (approx. 3 mol%) by using $EuCl_2$. Owing to the air-sensitivity, the starting materials were handled in an Ar-filled glovebox (Unilab, MBraun, Garching, $O_2 <$ 1 ppm, $H_2O < 0.1$ ppm), ground in an agate mortar and transferred into a cylindrical h-BN crucible (HeBoSint® S100, Henze, Kempten, Germany) and closed by a h-BN cap. The latter was placed in an octahedron ($MgO:Cr_2O_3$ (5%), edge length 18 mm, Ceramic Substrates & Components, Isle of Wight, UK), which was drilled through and loaded with a ZrO_2 sleeve (Cesima Ceramics, Wust-Fischbeck, Germany), which contains graphite tubes (Schunk Kohlenstofftechnik GmbH, Gießen, Germany) as electrical resistance furnaces. As pressure media Co-doped (7%) WC cubes (Hawedia, Marklkofen, Germany) with truncated edges (edge length 11 mm) were used. This elaborate design results in a homogeneous pressure transfer to the sample. Additional information regarding this high-pressure setup may be found in the literature.[65,66] The related synthesis conditions can be found in the synthesis part of Results and Discussion.

Scanning Electron Microscopy (SEM) with Energy-Dispersive X-ray Spectroscopy (EDX): Studies of morphology and chemical compositions of the title compounds were performed on a dual-beam Helios Nanolab G3 UC (FEI, Hillsboro) with an X-Max 80 SDD EDX detector (Oxford Instruments, Abingdon). For this purpose, analysis samples were fixed on carbon adhesive pads.

Solid-state magic angle spinning (MAS) NMR spectroscopy: ^{31}P NMR spectra were collected with a DSX AVANCE spectrometer (Bruker) with a magnetic field of 11.7 T. The β-$MgSrP_3N_5O_2$ sample was filled into a rotor with a diameter of 2.5 mm, which was mounted on a commercial MAS probe (Bruker). The sample was rotated at a rotation frequency of 20 kHz. The obtained data were analysed using device-specific software.

Single-crystal X-ray Diffraction (SCXRD): A Bruker D8 Quest diffractometer with Mo–K_α radiation ($\lambda = 0.71073$ Å) was used for data collection. SADABS was used for absorption correction.[67] The crystal structure was solved by direct methods (SHELXT) and refined by full-matrix least square methods (SHELXL).[68] Deposition number www.ccdc.cam.ac.uk/services/structures?id=doi:10.1002/chem.2023012182236964 (**β-$MgSrP_3N_5O_2$**) contains the supplementary crystallographic data for this paper. The data are provided free of charge by the joint Cambridge Crystallographic Data Centre and Fachinformationszentrum Karlsruhe Access Structures service (http://www.ccdc.cam.ac.uk/structures).

Powder X-ray Diffraction (PDXRD): Powder X-ray measurements were performed by using a STOE STADI P diffractometer with Cu-$K_{\alpha1}$ radiation ($\lambda = 1.5406$ Å), Ge(111) monochromator and Mythen 1 K detector in modified Debye-Scherrer geometry. The samples were sealed in a glass capillary (0.3 mm, Hilgenberg GmbH). The obtained data were Rietveld refined using TOPAS.[69]

Quantum-Chemical Calculations: Periodic density-functional theory (DFT) calculations were performed using the Vienna ab initio simulation package (VASP).[70] Core and valence electrons were separated using projector-augmented waves (PAW).[71] Generalized-gradient approximation as described by Perdew, Burke and Ernzerhof (GGA-PBE) was used for the treatment of the exchange and correlation contributions.[72,73] Additional corrections for van-der-Waals forces were included using the DFT-D3 method with Becke–Johnson dumping function.[74,75] The Brillouin zone was sampled on a Γ-centred k-point grid (α-$MgSrP_3N_5O_2$: 5×5×3 β-$MgSrP_3N_5O_2$: 4×2×6). The energy convergence criterium was set to 10^{-6} eV and the residual atomic forces were relaxed until the convergence criterion of $2\cdot10^{-2}$ eV/Å was reached. The energy versus volume data was computed by scaling the cell parameters from 95 to 105% (fixed $a:b:c$ ratio). The enthalpy as a function of the pressure was obtained by fitting the energy versus volume data to the Universal Equation of State.[44]

Acknowledgements

The authors gratefully acknowledge the computational and data resources provided by the Leibniz Supercomputing Centre (www.lrz.de). We also thank Dr. Lisa Gamperl and Amalina Buda for carrying out SEM-EDX measurements and Christian Minke for NMR measurements. Furthermore, we thank Kristian Witthaut (all at Department of Chemistry at LMU Munich) for inspiring discussions. Open Access funding enabled and organized by Projekt DEAL.

Conflict of Interests

The authors declare no conflict of interest.

Data Availability Statement

The data that support the findings of this study are available in the supplementary material of this article.

Keywords: high-pressure chemistry · luminescence · nitrides · oxonitridophosphates · solid-state structures

[1] S. Wendl, M. Mallmann, P. Strobel, P. J. Schmidt, W. Schnick, *Eur. J. Inorg. Chem.* **2020**, *841*.
[2] A. Marchuk, P. Schultz, C. Hoch, O. Oeckler, W. Schnick, *Inorg. Chem.* **2016**, *55*, 974.
[3] S. J. Sedlmaier, J. Schmedt auf der Günne, W. Schnick, *Dalton Trans.* **2009**, 4081.
[4] Y. Q. Li, A. C. A. Delsing, G. De With, H. T. Hintzen, *Chem. Mater.* **2005**, *17*, 3242.
[5] F. Wang, W. Wang, L. Zhang, J. Zheng, Y. Jin, J. Zhang, *RSC Adv.* **2017**, *7*, 27422.
[6] M. Bykov, E. Bykova, V. Dyadkin, D. Baumann, W. Schnick, L. Dubrovinsky, N. Dubrovinskaia, *Acta Crystallogr. Sect. E* **2015**, *71*, 1325.
[7] D. Baumann, S. J. Sedlmaier, W. Schnick, *Angew. Chem. Int. Ed.* **2012**, *51*, 4707; *Angew. Chem.* **2012**, *124*, 4785.
[8] H. Huppertz, O. Oeckler, A. Lieb, R. Glaum, D. Johrendt, M. Tegel, R. Kaindl, W. Schnick, *Chem. Eur. J.* **2012**, *18*, 10857.
[9] S. J. Sedlmaier, E. Mugnaioli, O. Oeckler, U. Kolb, W. Schnick, *Chem. Eur. J.* **2011**, *17*, 11258.
[10] H. Daicho, Y. Shinomiya, A. Nakano, H. Sawa, S. Matsuishi, H. Hosono, *Chem. Commun.* **2018**, *54*, 884.
[11] S. Horstmann, E. Irran, W. Schnick, *Angew. Chem. Int. Ed. Engl.* **1997**, *36*, 1873; *Angew. Chem.* **1997**, *109*, 1938.
[12] M. Nentwig, S. D. Kloß, L. Neudert, L. Eisenburger, W. Schnick, O. Oeckler, *Chem. Eur. J.* **2019**, *25*, 14382.
[13] D. Günther, L. Eisenburger, W. Schnick, O. Oeckler, *Z. Anorg. Allg. Chem.* **2022**, 648, e202200280.
[14] F. J. Pucher, W. Schnick, *Z. Anorg. Allg. Chem.* **2014**, *640*, 2708.
[15] F. Karau, W. Schnick, *Z. Anorg. Allg. Chem.* **2006**, *632*, 231.
[16] L. Eisenburger, V. Weippert, C. Paulmann, D. Johrendt, O. Oeckler, W. Schnick, *Angew. Chem. Int. Ed.* **2022**, *61*, e202202014; *Angew. Chem.* **2022**, *134*, e202202014.
[17] L. Eisenburger, V. Weippert, O. Oeckler, W. Schnick, *Chem. Eur. J.* **2021**, *27*, 14184.
[18] S. D. Kloß, N. Weidmann, R. Niklaus, W. Schnick, *Inorg. Chem.* **2016**, *55*, 9400.
[19] R. Marchand, A. Jayaweera, P. Verdier, J. Lang, *C. R. Acad. Sci., Ser. C* **1976**, *283*, 675.
[20] S. J. Sedlmaier, D. Weber, W. Schnick, *Z. Kristallogr. - NCS* **2012**, *227*, 1.
[21] B. E. Warren, *Z. Kristallogr. – Cryst. Mater.* **1930**, *74*, 131.
[22] J. M. S. Skakle, R. Herd, *Powder Diffr.* **1999**, *14*, 195.
[23] V. V. Brazhkin, Y. Katayama, A. G. Lyapin, H. Saitoh, *Phys. Rev. B* **2014**, *89*, 104203.
[24] S. Correll, N. Stock, O. Oeckler, J. Senker, T. Nilges, W. Schnick, *Z. Anorg. Allg. Chem.* **2004**, *630*, 2205.
[25] S. Schneider, L. G. Balzat, B. V. Lotsch, W. Schnick, *Chem. Eur. J.* **2023**, *29*, e202202984.
[26] E.-M. Bertschler, R. Niklaus, W. Schnick, *Chem. Eur. J.* **2018**, *24*, 736.
[27] E.-M. Bertschler, R. Niklaus, W. Schnick, *Chem. Eur. J.* **2017**, *23*, 9592.
[28] S. M. Clarke, K. M. Powderly, J. P. S. Walsh, T. Yu, Y. Wang, Y. Meng, S. D. Jacobsen, D. E. Freedman, *Chem. Mater.* **2019**, *31*, 955.
[29] F. Liebau, *Structural Chemistry of Silicates: Structure, Bonding, and Classification*, Springer, Heidelberg, **1985**, 62.
[30] K. Momma, F. Izumi, *J. Appl. Crystallogr.* **2011**, *44*, 1272.
[31] L. Pauling, *J. Am. Chem. Soc.* **1929**, *51*, 1010.
[32] P. E. D. Morgan, *J. Mater. Sci.* **1986**, 4305.
[33] A. Fuertes, *Inorg. Chem.* **2006**, *45*, 9640.
[34] R. Hoppe, *Z. Naturforsch. A* **1995**, *6*, 555.

[35] R. Hoppe, S. Voigt, H. Glaum, J. Kissel, H. P. Müller, K. Bernet, *J. Less-Common Met.* **1989**, *156*, 105.
[36] I. D. Brown, D. Altermatt, *Acta Crystallogr. Sect. B* **1985**, *41*, 244.
[37] N. E-Brese, M. O'Keefe, *Acta Crystallogr. Sect. B* **1991**, *47*, 192.
[38] A. Altomare, C. Cuocci, C. Giacovazzo, A. Moliterni, R. Rizzi, N. Corriero, A. Falcicchio, *J. Appl. Crystallogr.* **2013**, *46*, 1231.
[39] M. O'Keeffe, M. A. Peskov, S. J. Ramsden, O. M. Yaghi, *Acc. Chem. Res.* **2008**, *41*, 1782.
[40] V. A. Blatov, A. P. Shevchenko, D. M. Proserpio, *Cryst. Growth Des.* **2014**, *14*, 3576.
[41] J.-M. Du, H.-Y. Zeng, L.-J. Song, Z.-C. Dong, H.-W. Ma, G.-C. Guo, J.-S. Huan, *Chinese J. Struct. Chem.* **2003**, *22*, 33.
[42] R. D. Shannon, *Acta Crystallogr. Sect. A* **1976**, *32*, 751.
[43] A. Neuhaus, *Chimia* **1964**, *18*, 93.
[44] P. Vinet, J. H. Rose, J. Ferrante, J. R. Smith, *J. Phys. Condens. Matter* **1989**, *1*, 1941.
[45] R. López, R. Gómez, *J. Sol-Gel Sci. Technol.* **2012**, *61*, 1.
[46] J. Tauc, R. Grigorovici, A. Vancu, *Phys. Status Solidi B* **1966**, *15*, 627.
[47] M.-H. Fang, C. O. M. Mariano, P.-Y. Chen, S.-F. Hu, R–S. Liu, *Chem. Mater.* **2020**, *32*, 1748.
[48] J. A. Kechele, O. Oeckler, F. Stadler, W. Schnick, *Solid State Sci.* **2009**, *11*, 537.
[49] O. Oeckler, F. Stadler, T. Rosenthal, W. Schnick, *Solid State Sci.* **2007**, *9*, 205.
[50] M. Seibald, T. Rosenthal, O. Oeckler, W. Schnick, *Crit. Rev. Solid State Mater. Sci.* **2014**, *39*, 215.
[51] X. Zhang, M.-H. Fang, Y.-T. Tsai, A. Lazarowska, S. Mahlik, T. Lesniewski, M. Grinberg, W. K. Pang, F. Pan, C. Liang, W. Zhou, J. Wang, J.-F. Lee, B.-M. Cheng, T.-L. Hung, Y.-Y. Chen, R.-S. Liu, *Chem. Mater.* **2017**, *29*, 6781.
[52] A. Kitai, *Materials for Solid State Lighting and Displays*, John Wiley and Sons, Chichester, **2017**.
[53] R.-J. Xie, Y. Q. Li, N. Hirosaki, H. Yamamoto, *Nitride Phosphors and Solid-State Lighting*, Taylor & Francis, Boca Raton, **2011**.
[54] L. Eisenburger, O. Oeckler, W. Schnick, *Chem. Eur. J.* **2021**, *27*, 4461.
[55] R. S. Hafei, D. Maganas, P. Strobel, P. J. Schmidt, W. Schnick, F. Neese, *J. Am. Chem. Soc.* **2022**, *144*, 8038.
[56] P. Strobel, T. de Boer, V. Weiler, P. J. Schmidt, A. Moewes, W. Schnick, *Chem. Mater.* **2018**, *30*, 3122.
[57] High Color-Rendering, Full-Visible-Spectrum LEDs by Soraa. *LED professional Review* **2016**.
[58] A. Stock, H. Grüneberg, *Ber. Dtsch. Chem. Ges.* **1907**, *40*, 2573.
[59] K. J. Kingma, R. G. Pacalo, P. F. McMillan, *Eur. J. Solid State Inorg. Chem.* **1997**, *24*, 679.
[60] R. Suhrmann, K. Clusius, *Z. Anorg. Allg. Chem.* **1926**, *152*, 52.
[61] F. W. Karau, *Dissertation*, Ludwig-Maximilians-Universität München (Germany) **2007**.
[62] D. Walker, M. A. Carpenter, C. M. Hitch, *Am. Mineral.* **1990**, *75*, 1020.
[63] D. Walker, *Am. Mineral.* **1991**, *76*, 1092.
[64] D. C. Rubie, *Phase Transitions* **1999**, *68*,431.
[65] H. Huppertz, *Z. Kristallogr.* **2004**, *219*, 330.
[66] N. Kawai, S. Endo, *Rev. Sci. Instrum.* **1970**, *41*, 1178.
[67] Bruker AXS, Inc., *SADABS*, Madison, Wisconsin, USA, **2001**.
[68] G. M. Sheldrick, *Acta Crystallogr. Sect. C* **2015**, *71*, 3.
[69] A. A. Coelho, *TOPAS-Academic*, Version 6, Coelho Software, Brisbane (Australia), **2016**.
[70] Kresse, G. Furthmüller, *J. Comput. Mater. Sci.* **1996**, *6*, 15.
[71] P. E. Blöchl, *Phys. Rev. B: Condens. Matter Mater. Phys.* **1994**, *50*.
[72] J. P. Perdew, K. Burke, M. Ernzerhof, *Phys. Rev. Lett.* **1996**, *77*,3865.
[73] J. P. Perdew, J. P. K. Burke, M. Ernzerhof, *Phys. Rev. Lett.* **1997**, *78*,1396.
[74] S. Grimme, J. Antony, S. Ehrlich, H. Krieg, *J. Chem. Phys.* **2010**, *132*, 154104.
[75] S. Grimme, S. Ehrlich, L. Goerigk, *J. Comput. Chem.* **2011**, *32*, 1456.

Manuscript received: April 18, 2023
Accepted manuscript online: May 19, 2023
Version of record online: June 13, 2023